Type of the Paper: Research Article

β-adrenergic stimulation synchronizes a broad spectrum of action potential firing rates of cardiac pacemaker cells towards a higher population average

Mary S. Kim, Oliver Monfredi, Larissa A. Maltseva, Edward G. Lakatta and Victor A. Maltsev *

Laboratory of Cardiovascular Science, National Institute on Aging, NIH, Baltimore, MD 21224, USA
* Correspondence: maltsevvi@mail.nih.gov

Abstract: The heartbeat is initiated by pacemaker cells residing in the sinoatrial node (SAN). SAN cells generate spontaneous action potentials (APs), i.e. normal automaticity. The sympathetic nervous system increases heart rate commensurate with blood supply and cardiac output demand, known as the fight-or-flight response, *via* stimulation of SAN β-adrenergic receptors (βAR). It is classically believed that all cells increase their spontaneous AP firing rate in a similar fashion. In the present study we measured βAR responses among 166 single SAN cells isolated from 33 guinea pig hearts. However, the responses substantially varied. In each cell changes in AP cycle length in response to βAR stimulation highly correlated (R^2=0.97) with the AP cycle lengths before stimulation. While, as expected, on average the cells increased their pacemaker rate, greater responses were observed in cells with slower basal rates, and vice versa, cells with higher basal rates showed smaller responses, no responses, or even negative responses, i.e. their rate decreased. Thus, βAR stimulation synchronizes operation of the cell population towards a higher average rate, rather than uniformly shifting the rate in each cell, creating a new paradigm of fight-or-flight response among individual pacemaker SAN cells.

Keywords: Heart rate; automaticity; pacemaker; sinoatrial node cell; β-adrenergic receptors; fight-or-flight response; synchronization

1. Introduction

Enzymatically isolated single sinoatrial node (SAN) cells have been utilized as a model in studies of cellular mechanisms of cardiac pacemaker rate regulation [1]. This includes data on how cells respond to autonomic receptor stimulation: β-adrenergic receptors (βAR) increase spontaneous action potential (AP) firing rate in SAN, while cholinergic receptors decrease the rate, respectively. It is generally believed that βAR stimulation shifts AP firing rate in a similar fashion in all SAN cells *via* a small increase in the slope of diastolic depolarization [2]. The idea of the rate shift is based on electrophysiological measurements performed in a relatively small population of cells (believed to represent "true" or "healthy" pacemaker cells) that beat frequently and rhythmically after their enzymatic isolation, similar to the behavior of the whole SA node. However, only 10-30% of isolated cells contracted spontaneously in the original paper describing SAN cell isolation by Nakayama et al. [3]. The SAN cell isolation procedure has been substantially refined and improved since 1984, and the yield of spontaneously and rhythmically contracting cells has increased respectively but has never approached 100%. In addition to cells firing frequent and rhythmic spontaneous APs, many isolated cells fire APs at low and irregular rates, while others remain silent and do not beat at all despite a normal appearance.

Traditional research focusing only on "healthy", frequently beating SAN cells is justified on the basis of the operational paradigm that pacemaker SAN tissue is led by a leading pacemaker cell (or a cell cluster), dictating

the excitation rate and rhythm to all other subservient cells [4,5]. Coordinated firing of individual cells within SAN tissue has also been approached along the lines of mutual entrainment of individual cells towards a single rate within a network of loosely coupled oscillators (dubbed the 'democratic process') [6,7]. Thus, historical single cell studies have preferred to choose and make measurements in SAN cells that are spontaneously beating after isolation, with rates and rhythms similar to that of intact SAN tissue. All other cells that do not fit this paradigm, i.e. non-beating, irregular or infrequently beating cells, were usually rejected for further study on the basis that they were likely damaged by the enzymatic isolation procedure, or that they were subsidiary pacemaker cells, i.e. not the "true" pacemaker cells.

This "one rate/rhythm" paradigm of SAN cell operation and related criteria of pacemaker cell vitality and authenticity has recently been challenged. Using a novel high-resolution imaging technique, Bychkov et al. [8] recorded Ca signals in individual cells over the entire intact mouse SAN and found that synchronized cardiac impulses emerge from heterogeneous local Ca signals within and among cells of pacemaker tissue, resembling complex processes of impulse generation within clusters of neurons in neuronal networks. An important observation was that many cells within the HCN4-positive network (where pacemaker impulses first emerge) do not generate APs or generate APs with rates and rhythms different from those exiting the SAN to capture the atria. Another recent study by Fenske et al. [9] in knock-in mice expressing cAMP-insensitive HCN4 channels showed that tonic and mutual interaction (so-called 'tonic entrainment') between firing and non-firing cells slows down pacemaking in the SAN, and that cAMP increases the proportion of firing cells, and in doing so increases the rate of SAN automaticity, and also increases resistance to parasympathetic stimulation.

We have recently examined non-firing, silent cells, dubbed dormant cells, isolated from guinea pig and human hearts [10-12]. Many dormant cells can be reversibly "awakened" to fire normal, spontaneous rhythmic APs during βAR stimulation. The transition to spontaneous AP firing occurs *via* the emergence and coupling of rhythmic intracellular Ca oscillations (known as the Ca clock [13,14]), generating rhythmic local Ca releases (LCRs), with the membrane oscillator (known as the membrane clock), generating high-amplitude APs. During the transition to AP firing, the clocks' functions undergo specific changes that include: (i) increased cAMP activating I_f; (ii) increased cAMP-mediated phosphorylation of phospholamban increasing I_{CaL} density and accelerating Ca pumping; (iii) increased spatiotemporal LCR synchronization, yielding a larger diastolic LCR ensemble signal and an earlier increase in diastolic Na/Ca exchanger current [12]. All these changes result in effective AP ignition required for clock coupling during diastolic depolarization [15].

While cAMP-dependent phosphorylation is a key regulator of clock coupling [16], how different degrees of phosphorylation translate in clock coupling and specific cell behaviors (e.g. dormancy, rhythmic or dysrhythmic firing, autonomic receptor modulation, etc.) will depend on the expression level of clock proteins in individual cells. This cannot be assumed to be the same from cell to cell - immunocytochemical labeling of the L-type Ca channels, Na/Ca exchanger, Ca release channels (RyR2), and Ca pump (SERCA2) varies widely in SAN cells [17]. SAN cells also exhibit substantial degree of cell-to-cell variability in functional expression of I_{CaL}, I_f, and I_K [18,19]. For example, cell-to-cell variations in I_{CaL} or I_f densities can be as much as an order of magnitude. LCRs also vary substantially in different cells, with their period highly correlating with the AP cycle length [20]. Thus, we propose that enzymatically isolated SAN cells have a wide spectrum of basal beating rates (high rates to dormancy) as well as responses to βAR stimulation, due to natural diversity rather than damage during isolation procedure.

The present study, for the first time, has comprehensively examined responses to βAR stimulation in all AP firing cells to assess the overall reaction of the entire population of isolated cells. We hypothesized that beating response would vary substantially among cells, and that this would be dependent on their basal rates. We found that cell responses to βAR stimulation differed fundamentally from the dogma that all cells increase their rate in a similar fashion. While the majority of cells increased their rate, some cells were insensitive to stimulation, while others even paradoxically decreased their rates. Overall, during βAR stimulation, the spectrum of rates among individual cells substantially narrowed and became synchronized towards a higher average.

2. Materials and Methods

2.1. Single cell preparation

SAN cells were isolated from 33 male guinea pigs in accordance with NIH guidelines for the care and use of animals, protocol 034-LCS-2019 [10]. Hartley guinea pigs (Charles River Laboratories, USA) weighing 500-650 g were anesthetized with sodium pentobarbital (50–90 mg/kg). The heart was removed quickly and placed in solution containing (in mM): 130 NaCl, 24 $NaHCO_3$, 1.2 NaH_2PO_4, 1.0 $MgCl_2$, 1.8 $CaCl_2$, 4.0 KCl, 5.6 glucose equilibrated with 95% O_2 / 5% CO_2 (pH 7.4 at 35°C). The SA node region was cut into small strips (~1.0 mm wide) perpendicular to the crista terminalis and excised. The final SA node preparation consisted of SA node strips attached to the small portion of crista terminalis. The SA node preparation was washed twice in Ca-free solution containing (in mM): 140 NaCl, 5.4 KCl, 0.5 $MgCl_2$, 0.33 NaH_2PO_4, 5 HEPES, 5.5 glucose, (pH=6.9) and incubated on a shaker at 35°C for 30 min in the same solution with the addition of elastase type IV (0.6 mg/ml; Sigma, Chemical Co.), collagenase type 2 (0.8 mg/ml; Worthington, NJ, USA), protease XIV (0.12 mg/ml; Sigma, Chemical Co.), and 0.1% bovine serum albumin (Sigma, Chemical Co.). The SAN preparation was washed in modified Kraftbruhe (KB) solution, containing (in mM): 70 potassium glutamate, 30 KCl, 10 KH_2PO_4, 1 $MgCl_2$, 20 taurine, 10 glucose, 0.3 EGTA, and 10 HEPES (titrated to pH 7.4 with KOH), and kept at 4°C for 1h in KB solution containing 50 mg/ml polyvinylpyrrolidone (Sigma, Chemical Co.). Finally, cells were dispersed from the SA node preparation by gentle pipetting in the KB solution and stored at 4°C for subsequent use in our experiments for 8 hours.

2.2. Two-dimensional (2D) Ca imaging of single cells

Ca dynamics within isolated single SAN cells were measured by 2D imaging of fluorescence emitted by the Ca indicator Fluo-4 (Invitrogen) using a Hamamatsu C9100-12 CCD camera (100 frames/sec), with an 8.192 mm square sensor of 512 X 512 pixels resolution), as previously described [21]. The camera was mounted on a Zeiss Axiovert 100 inverted microscope (Carl Zeiss, Inc., Germany) with x63 oil immersion lens and a fluorescence excitation light source CoolLED pE-300-W (CoolLED Ltd. Andover, UK). Fluo-4 fluorescence excitation (blue light, 470/40 nm) and emission light collection (green light, 525/50 nm) were performed using the Zeiss filter set 38 HE. Cells were loaded with 5 mM Fluo-4AM (Sigma-Aldrich, USA) for 20 minutes at room temperature. The physiological (bathing) solution contained (in mM): 140 NaCl; 5.4 KCl; 2 $MgCl_2$; 5 HEPES; 1.8 $CaCl_2$; pH 7.3 (adjusted with NaOH). Data acquisition was performed using SimplePCI (Hamamatsu Corporation, Japan) at physiological temperature of 35°C ± 0.1°C.

2.3. Detection and analysis of the whole ensemble of AP-induced cytosolic Ca transients and LCRs in 2D Ca imaging

AP-induced Ca transients were observed as sharp, whole-cell wide (i.e. within the entire cell perimeter) transient rises of Fluo-4 fluorescence. We considered the time periods between these high amplitude signals as a satisfactory measure of AP cycle length (further referred as cycle length) as we previously reported in simultaneous recordings of Ca and membrane potential [22]. The time series of whole-cell Fluo-4 fluorescence (within the cell perimeter) were measured from 2D video recordings using HCImageLive image analysis software (v.3, x64, Hamamatsu Co., Japan). Then fluorescence peaks (i.e. AP-induced Ca transients) and their respective cycle lengths were determined by our custom-made program (Victor Maltsev).

LCRs were observed as local Ca signals scattered within cell perimeter. They were detected and analyzed by program "XYT Event Detector" [23] (its C++ code is freely available on NIH website https://www.nia.nih.gov/research/labs/xyt-event-detector)

In short, the program detects LCR birth/death events by a differential, frame-to-frame sensitivity algorithm applied to each pixel (cell location) in a series of images generated by the camera. An LCR is detected when its signal changes sufficiently quickly within a sufficiently large area. The LCR "dies" when its amplitude decays substantially or when it merges into a rising AP-induced Ca transient. LCRs were isolated from noise by applying a series of spatial filters that set the minimum pixel size and the brightness threshold for LCRs. Cells with mechanical contractile movements were affixed by tracking points along the midline of the moving cell by using a computer program "SANC Analysis" described in [23]. The algorithm uses these points as a coordinate system for affine transform, producing a transformed image series that are stationary. The program is available as a free

ImageJ plugin on the website http://scepticalphysiologist.com/code/code.html created and maintained by Dr. Sean Parsons.

2.4. Evaluation of βAR stimulation effect

βARs were stimulated by 1 μM isoproterenol in SAN cells during their continuous perfusion with physiological solution. To avoid photodamage, Ca signals were measured shortly, within 30 seconds before βAR stimulation (designated as control or basal state) and in the presence of stimulation approximately 5 minutes after isoproterenol application onset. The cycle lengths were measured (as described above) and each measured cell was represented by two numbers: average cycle lengths in control and in the presence of βAR stimulation. We also evaluated effect of βAR stimulation on LCR characteristics, namely: LCR period, time from AP-induced Ca transient peak to the onset of an LCR (ms); LCR duration, time from LCR onset to its "death" or merging to the transient (ms); LCR area, the cell area that was covered by a given LCR during its life span including expansion and propagation (μm^2) (reflecting parameter "LCR spatial size" reported in confocal line-scan images [20]); maximum LCR size, the area of the largest LCR in each cycle (μm^2).

2.5. Statistics

Data are presented as mean ± SEM. The statistical significance of the effects of βAR stimulation on cycle length and LCR characteristics was evaluated by pared T-test (n=166, in each cell before and during stimulation).

3. Results

3.1. Cycle length changes

On average, SAN cells significantly decreased their spontaneous cycle length in response to βAR stimulation. Statistical evaluation of the responses is provided in Table 1.

Table 1. Effect of βAR stimulation on cycle length measured in a population of 166 SAN cells that generated spontaneous AP-induced Ca transients; SEM, standard error of mean; SD, standard deviation, CV%= 100%* SD/Mean, coefficient of variation.

Parameter	Before stimulation	βAR stimulation
Mean cycle length, ms	921.8[1]	507.3[1]
SEM, ms	66.5	13.1
SD, ms	856.4	169.1
CV%	92.9	33.3

[1] Statistically significant with P<0.001 *via* pared t-Test, two tail.

However, the responses varied substantially from cell to cell and can be categorized into three types: (i) The majority of cells, 121 of 166 (72.9%) showed a “classical” response of cycle length reduction, i.e. their rate increased; (ii) a relatively small fraction of cells, 12 of 166 (7.2%) showed almost no change of the cycle length (within 3%); (iii) the rest of the tested cells, 33 of 166 (19.9%) showed an “unusual” or “paradoxical” response of cycle length increase (AP firing rates decrease). Examples of the responses in each category are shown in Figure 1 and respective Videos S1-S6 (each response category is presented by two video recordings: before and during βAR stimulation.

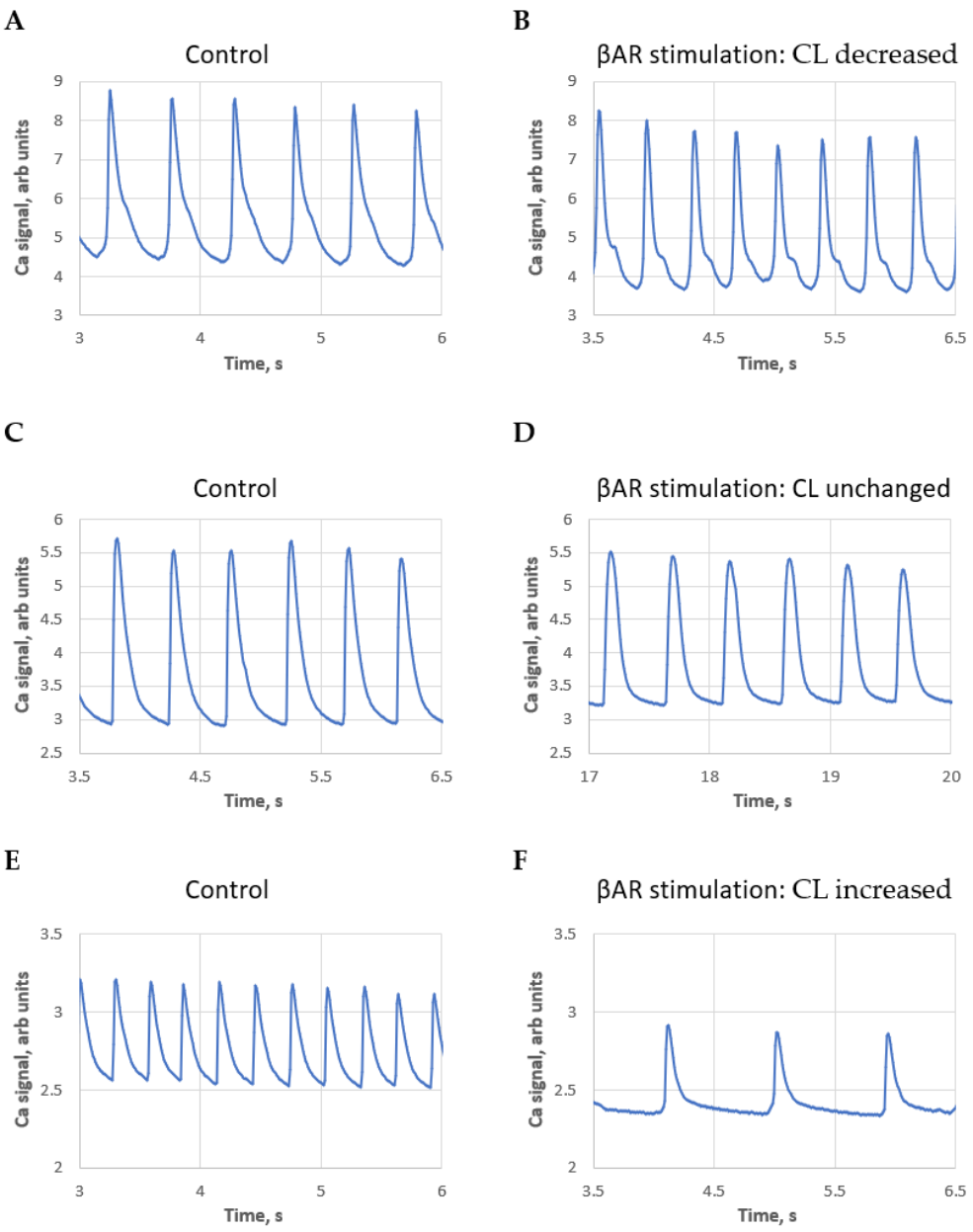

Figure 1. Examples of three types of βAR stimulation effects on AP-induced Ca transient cycle length (CL): (A,B): decrease; (C,D): no change; and (E,F): increase. All traces have the same 3s duration for clear visual comparison. See also respective Videos 1-6 of cell Ca dynamics in conrtol and in the presence of βAR stimulation.

We noticed that the classical response (positive in terms of AP rate increase) was observed in SAN cells with larger basal cycle length, whereas the paradoxical cycle length increases were mainly present in cells with a baseline short cycle length, i.e. in the cells that had higher rates in the basal state. The largest cycle length shortenings were observed in cells operating at extremely long cycle lengths (Figure 2, Videos 7 and 8), i.e. in SAN cells bordering the dormant state [10-12].

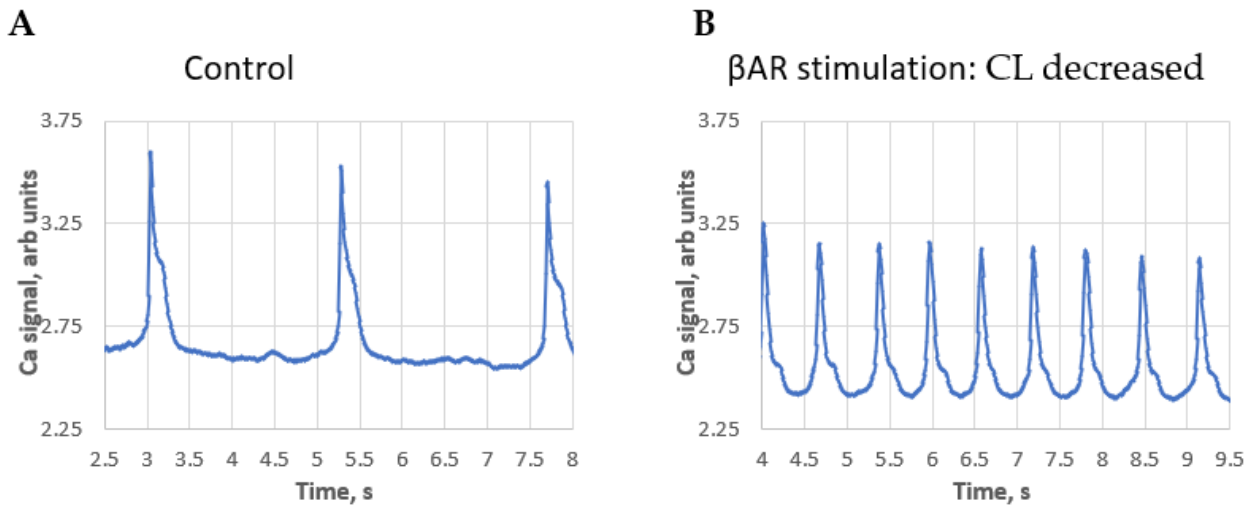

Figure 2. An example of βAR stimulation effect in cells with extremely long AP-induced Ca transient cycle length (CL). (A): at the base line, i.e. “almost dormant cell”. (B): βAR stimulation. Both traces have the same 5.5 s duration for clear visual comparison. See also respective Videos 7-8 of cell Ca dynamics in conrtol and in the presence of βAR stimulation.

We illustrated and statistically evaluated this result by plotting all responses together as a relationship of cycle length change vs. initial cycle length before βAR stimulation for each cell tested (Figure 3), The relationship was closely described by a linear function with R^2=0.961 indicating a strong correlation between the two. The fitted line crossed the x axis at a cycle length of 491 ms ("no change" cycle length), providing an approximate border between negative and positive responses that is also close to the average cycle length 507 ms in the presence of βAR stimulation, pointing to synchronization (or grouping) of the responses around this no-change cycle length value. Such synchronization is also evidenced by substantially smaller standard deviation of cycle lengths in stimulated cells and furthermore by substantially smaller coefficient of variation (CV) (33% vs. 93%, Table 1) of cycle length in the tested cell population in the presence of βAR stimulation.

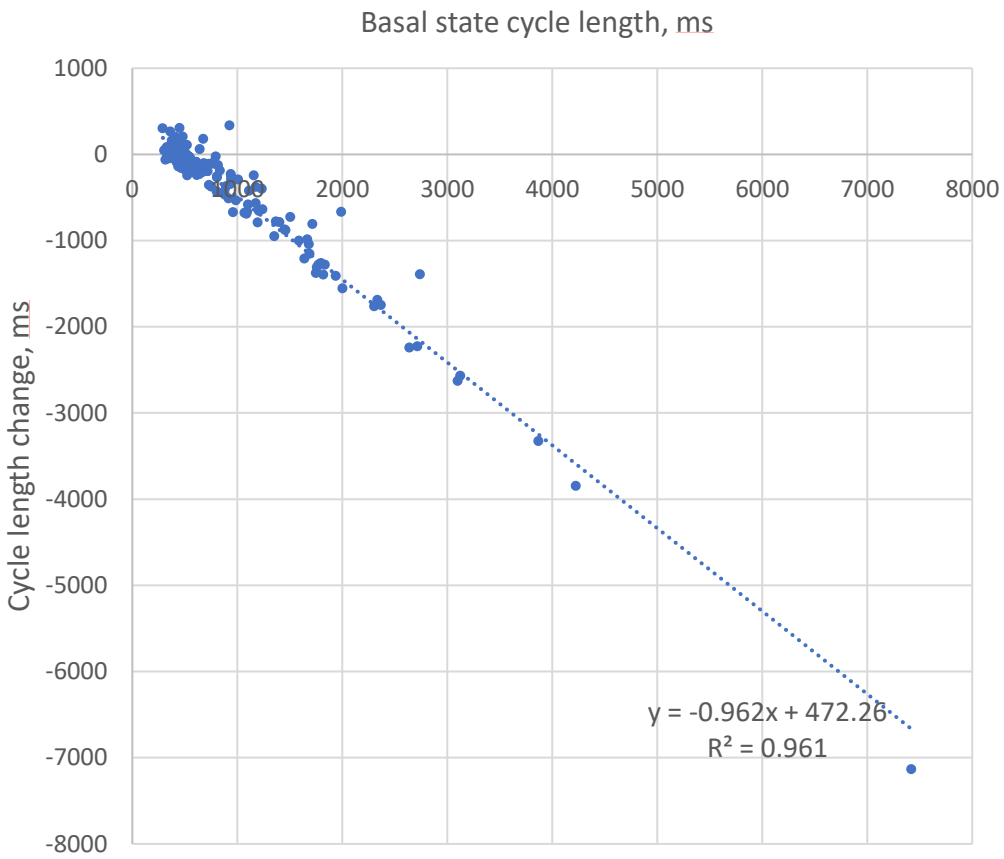

Figure 3. Strong correlation of the initial cycle length (basal state) with change in the cycle length in the presense of βAR stimulation. Negative numbers on Y axis represent cycle length decrease, i.e. rate increase.

The synchronization of cycle lengths in stimulated cells is clearly illustrated by comparison of the respective histograms for cycle lengths in control and in the presence of βAR stimulation (Figure 4). The cycle length distribution was spread widely in the basal state, with many cells exhibiting long, some extremely long values. In the presence of βAR stimulation the distribution substantially narrowed, with almost all cells operating around a common, higher (on average) rate.

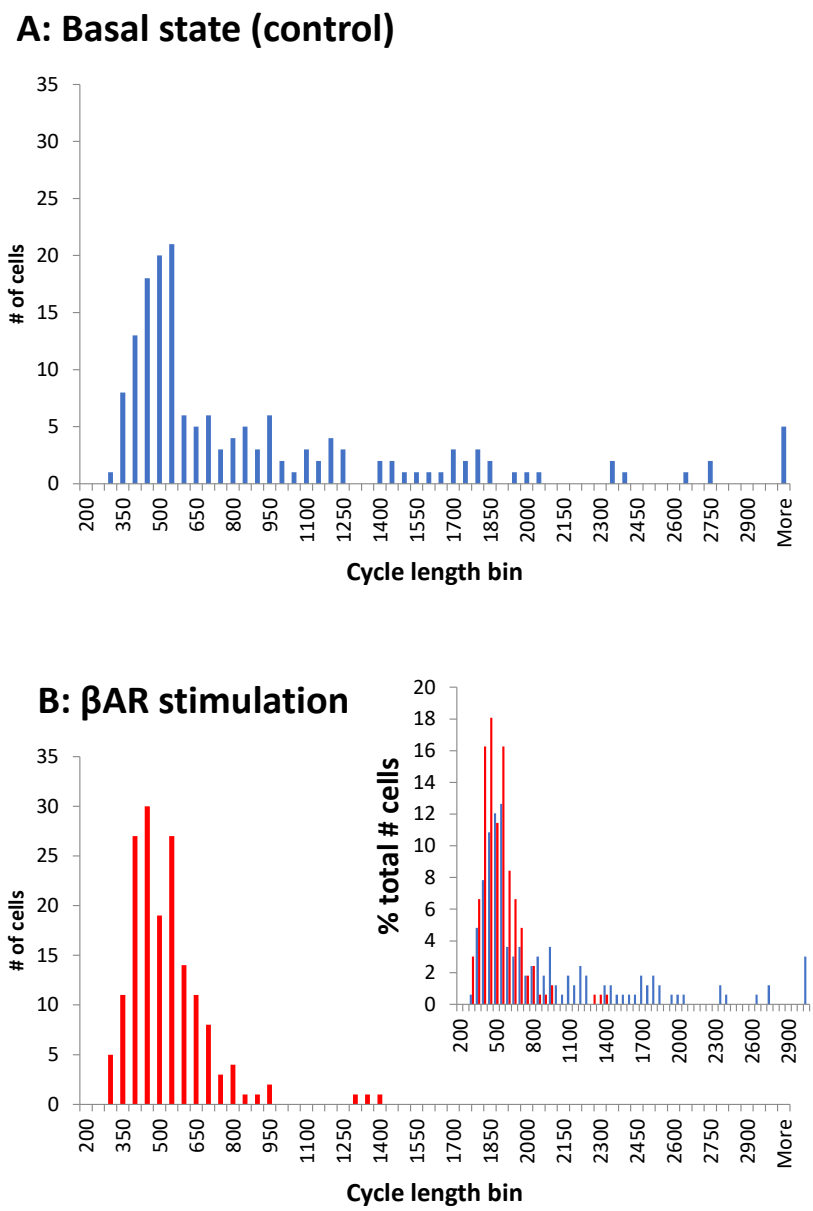

Figure 4. βAR stimulation synchronizes cell rates around a higher (on average) common rate, i.e. shorter cycle length. Histograms show cycle length distributions in 166 cells tested in the present study. Bin size is 50 ms. (A): in control. (B): in the presence of βAR stimulation. Inset: overlaping histograms in panels A and B expressed in terms of the percentage of cells in each cycle length bin illustrate a more narrow, synchrinized distribution of cycle lengths in stimulated cells (red) relative to control (blue).

3.2. LCR changes

Because our previous studies have shown the crucial importance of LCRs for βAR stimulation effect in AP firing SAN cells [24] as well as in dormant SAN cells [10-12], we also generated additional insights into the variability of the responses observed in this study by measuring and comparing changes in key LCR characteristics in cells responding with cycle length decrease vs. those with cycle length increase. All key LCR characteristics in SAN cells responding with cycle length decrease changed substantially (Figure 5) in line with the coupled-clock theory (see more in Discussion). In contrast, LCR characteristics in cells with cycle length increase showed no significant changes, except in LCR period, which increased (Figure 6).

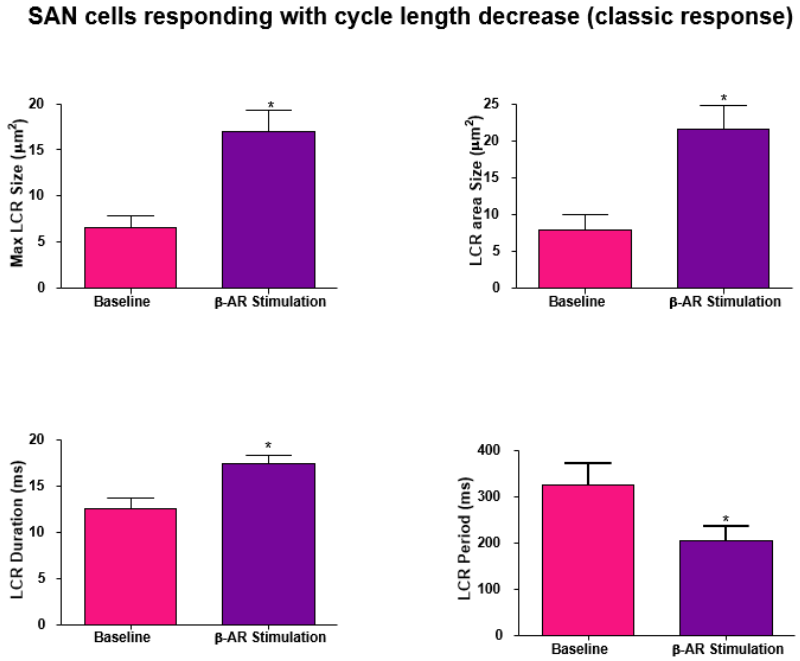

Figure 5. All measured LCR characteristics substantially and significantly change in cells with cycle lengh decrease (rate increase, i.e. classic response). *P<0.05, n=4 cells.

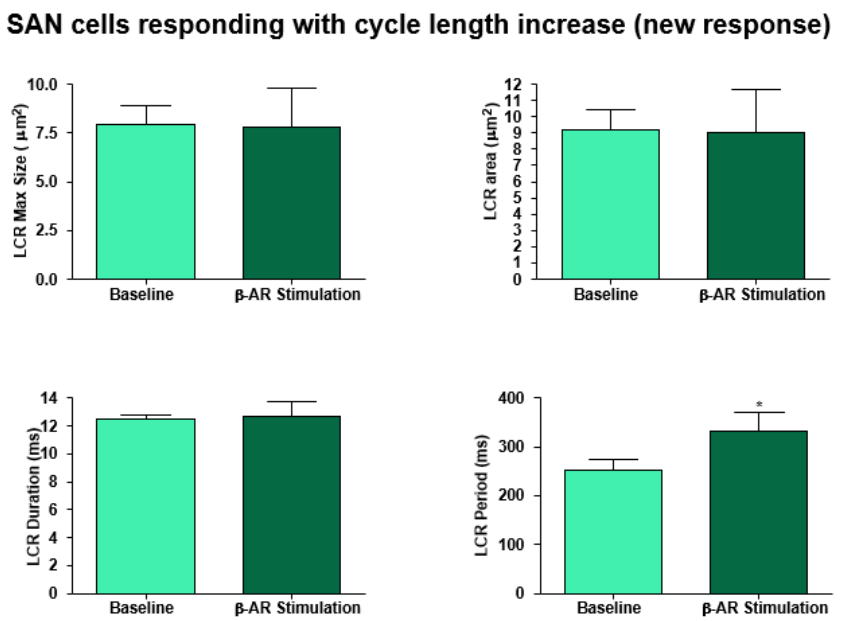

Figure 6. LCR characteristics do not change, except LCR period, in cells responding with the cycle length increase (rate decrease, i.e. a new response type). * P<0.05, n=5 cells

4. Discussion

4.1. Result summary

The present study, for the first time, examined the effect of βAR stimulation in a large number of pacemaker cells (n=166) isolated from the SAN of guinea pigs. Previous studies evaluated the average effect of βAR stimulation in an average cell within a small population of cells that were spontaneously beating after isolation with a rate similar to that of the intact SAN. Given recent findings in intact SAN [8,9] and in dormant cells [10-12], our new approach here was to examine βAR stimulation effects in a larger population of SAN cells generating spontaneous AP-induced Ca transients at any rate, including very low rates, bordering with dormancy. We tested the hypothesis that the responses would vary substantially among cells and endeavored to find a general relationship of the rate change during βAR stimulation among cells of the entire diverse population of cells. We found that βAR stimulation responses indeed markedly varied, and that the cycle length change in each cell was highly correlated (R^2=0.97) with the cycle length before stimulation. While on average cycle length decreased, larger cycle length shortenings were observed in cells with longer cycle lengths before stimulation, and vice versa, cells with shorter cycle length showed smaller responses or even paradoxical cycle length increases (Figure 3). Thus, βAR stimulation synchronizes intrinsic operation of SAN cells towards a higher average rate that differed fundamentally from a uniform shift in each cell as previously thought [2].

4.2. Possible mechanisms underlying different cell sensitivity to βAR stimulation

The large spectrum of cell sensitivities to βAR stimulation is likely linked to extremely high heterogeneity of SAN cells with respect to their expression of key proteins (including Ca cycling proteins [17,25]), and ion current densities [17-19]. Indeed, our theoretical studies [26] employing wide range, multidimensional sensitivity analyses tested hundreds of thousands of numerical models with different yet realistic parameters of both Ca and membrane clocks, and demonstrated substantial variation in the ranges of βAR stimulation effect. A major conclusion (related to this study) was that the full physiological range of rates can be achieved only in SAN cell models that incorporate a Ca clock. The membrane and Ca clocks operate in synergy providing robust, flexible, and energy efficient spontaneous AP firing [13,26]. In mathematical terms, the Ca clock operates *via* a *criticality*

mechanism [27] employing phase-like transitions [28]; it is continuously but variably coupled to membrane clock that generates current/voltage oscillations *via* a *limit- cycle* mechanism [29]. The criticality mechanisms, in turn, are governed by a power law and self-similarity across wide scales [30]. Thus, nature harnesses these universal and synergetic mechanisms to effectively execute the wide range of autonomic modulation receptor stimulation [31] in species with substantially different heart rates [32].

The specific mechanism of the beating rate increase during βAR stimulation in our study is also likely linked to coupled-clock function as evidenced by respective changes in LCR characteristics (Figure 5): average LCR area, maximum LCR size and LCR duration increased, indicating a stronger interaction of LCRs with the membrane clock over a larger total interaction area with Na/Ca exchanger. This LCR-linked mechanism is similar to that we reported for βAR stimulation in dormant cells [10-12] (discussed in Introduction).

Some cells (mainly with high basal rate) responded with rate slowing during βAR stimulation (Figure 1E), with their LCR period significantly increasing (Figure 6). An increase in LCR period is a common feature of SAN cells that decrease their firing rate (e.g. LCR period increases in the presence of cholinergic receptor stimulation [33]). Thus, the rate decrease could be LCR-dependent due to shifted timing of LCR occurrences. Other LCR characteristics (assessing strength of LCR signal) remained unchanged (Figure 6), in stark contrast to cells that responded with a beating rate increase (Figure 5). This indicates that the Ca clock (and its coupling to the membrane clock) is tuned to operate differently in these cell populations. This tuning can be linked to specific settings of complex biochemical reactions (the "biochemical engine" of the cardiac pacemaker) determining cAMP balance and protein phosphorylation driving the Ca clock and the coupled-clock system [14]. The biochemical engine can be slowed down *via* appropriate settings of "brakes" including a wide spectrum of different types of adenylyl cyclases (e.g. Ca-inhibited types), phosphatases, and phosphodiesterases, their operating regimes, and interplay including local interactions, e.g. in microdomains [34,35]. Bradycardic mechanisms of the membrane clock that may contribute to the rate slowing include Ca-activated K channels and Ca-dependent inactivation of I_{CaL}.

4.3. A broader interpretation of our results towards the entire range of autonomic modulation, including dormant cells

In the broader context, our finding of βAR stimulation to synchronize intrinsic cell oscillations (i.e. spontaneous AP rates of cells in isolation) could be further extended towards the entire range of rates executed by autonomic modulation, including cholinergic receptor stimulation, but likely with the opposite effect to desynchronize cell function [31]. Indeed, in the basal state, the distribution of intrinsic rates is dispersed, but still has a notable peak (Figure 4, top panel). Cell synchronization within the cell population in the presence of βAR stimulation transforms the distribution into a single narrow peak (Figure 4, bottom panel). Cell desynchronization in the presence of cholinergic receptor stimulation would likely result in the opposite effect, i.e. a more disperse (disordered) distribution vs. that in the basal state. If this hypothetical synchronization/desynchronization mechanism of cell population redistribution is correct, one could expect that low-rate cells would become non-firing cells in the presence of cholinergic stimulation (following Fenske et al. hypothesis), whereas in the presence of βAR stimulation low-rate cells would become high-rate cells (present study, Figure 4) and non-firing/dormant cells become firing cells [10-12]. Thus, our broader interpretation of autonomic modulation mechanism at the level of cell population includes redistributions of intrinsic cell functions within the entire spectrum of rates, importantly, with the rate zero, i.e. dormant cells, representing an indispensable part of the spectrum. This view is fundamentally different from the old-standing dogma of rate regulation *via* "the pacemaker cell", i.e. a hypothetical, average SAN cell executing the entire range of autonomic modulation [36-40].

4.4. A broader interpretation of our results towards synchronization mechanisms of cell signaling in intact SAN: cell specialization and local control by autonomic system

The findings of the present study are in line with the results of a preliminary study (reported recently as an abstract [41]) that cells isolated from different SAN regions exhibit not only different basal rates, but also different sensitivity to βAR stimulation. Different cell sensitivity to βAR stimulation, in turn, suggests that some

cells specialize to execute heart rate increase. Indeed, recent studies discovered two competing right atrial pacemakers near the superior vena cava and the inferior vena cava, dubbed the superior SAN and inferior SAN, respectively-which preferentially control the fast and slow heart rates [42]. Some cells in the presence of cholinergic receptor stimulation become silent, contributing to rate decrease as proposed by Fenske et al. [9]. Still other areas could be unresponsive to acetylcholine [43]. Using small tissue pieces dissected from rabbit SA node, Opthof et al. [44] found that SA node pieces bordering the left atrium were quiescent when dissected, but became activated to fire APs in the presence of adrenaline or acetylcholine.

Thus, cell specialization to generate different rates and different sensitivity of cells to autonomic stimulation within the cellular network of intact SAN can be interpreted to indicate that the role of autonomic modulation is in fact to redistribute signaling (i.e. local control) within the cellular network to amplify the contribution and deliver oscillations of a particular rate generated by a specialized cell population towards the SAN output. Such signal amplification within intact SAN may be executed *via* stochastic resonance [45] and/or percolation phase transition [29]. Another potential amplification mechanism is linked to dynamic changes in SAN network itself, i.e. autonomic system-guided local control of dynamic signal channeling. Indeed, during βAR stimulation, some additional (multiple) signaling pathways can be created within the network, as more non-firing/dormant cells become firing cells. Thus, cells not only synchronize their intrinsic firing rates (present study), but also their synchronized firing is more robustly and synchronously delivered to SAN output within the tissue *via* the dynamic signal channeling. In contrast, some signal paths to SAN output can be blocked by temporary nonfiring/dormant cells during cholinergic response (in addition to the tonic entrainment mechanism of Fenske at al. [9]), but become available again in basal state firing. Such specialized cell population-based mechanism (autonomic system local control of signal channeling) is reflected by the classic phenomenon, known as the shift of the dominant leading pacemaker site [46].

Interestingly, respiration, as yet another vital rhythmic function of the body, arises from complex and dynamic neuronal interactions within a diverse neural microcircuit and pacemaker properties are not necessary for respiratory rhythmogenesis [47]. Thus, regulation of cardiac automaticity can also utilize, at least in part, such neural microcircuit mechanism. How specifically, cell specialization and different degrees of synchronization in intrinsic cell signaling would be guided/modulated by autonomic system (locally and over entire SAN) and translated into a higher or lower rate of impulses emanated from the SAN remains unknown and merits further studies. A problem with interpretation of cell population data to the network level at this moment is that the new paradigm of heterogeneous signaling (including subthreshold signals, non-firing cells, and cell operating at various rates) has been just recently proposed [8,9]. While it has been noted that cell signaling in SAN network resembles multiscale complex processes of impulse generation within clusters of neurons in neuronal networks [8], establishing exact mechanisms of this complex signaling represents the frontier of cardiac pacemaker research. Testing new ideas and establishing exact mechanisms require new theoretical modeling. Multicellular numerical models of SAN function have been developed in 1 dimension (as a linear chain of consecutive SAN cells) [48-53], in 2 dimensions [54-56] and even in 3 dimensions [57]. Those models have provided new insights about importance of cell interactions, but they have not tested importance of dormant cells (with their subthreshold signaling) [10-12], cells operating at low rates found in intact SAN [8], and autonomic modulation. Cell population data presented here can be helpful for future numerical studies of SAN tissue to decrease uncertainties in choosing cell model parameters.

4.5. Importance of beat-to-beat variability

While the present study was focused on the rate responses, another important aspect of function of SAN cells is their beat-to-beat variability that ultimately contributes to heartbeat rhythmicity. In addition to respective rate changes, βAR stimulation increases rhythmicity of AP firing (*via* cell firing synchronization), whereas cholinergic receptor stimulation decreases rhythmicity of spontaneous AP firing [31,58]. Furthermore, Ca and membrane potential transitions during APs are found to be self-similar to each other and to variability of AP firing intervals across the entire physiologic range of AP intervals during autonomic receptor stimulation [31]. In fact, the rate and rhythm are intrinsically linked to each other at each and all scale levels (single cells, tissue, and heart) [58]. The data of the present study provides a new insight into this phenomenon. Indeed, if the SAN rate

and rhythm result from an integration (whatever it is) of signals from many or all cells, the network of cells with more narrow distribution of intrinsic rates in the presence of βAR stimulation (Figure 4), would logically give less variability at the output after the integration. Thus, future experimental studies of diverse populations of SAN cells and respective theoretical approaches will be more enlightening and effective if they include both rate and rhythm considerations.

4.6. Functional benefits of heterogeneity at tissue level

As noted, SAN cells exhibit extremely heterogeneous morphological, biophysical, and biochemical properties. Then what are the benefits and importance of this heterogeneity among cells within the SAN tissue? A comprehensive summary of thoughts in this regard was presented about 20 years ago in a seminal review by Boyett et al. [46] that concluded: "The heterogeneity is important for the dependable functioning of the SA node as the pacemaker for the heart, because (i) *via* multiple mechanisms, it allows the SA node to drive the surrounding atrial muscle without being suppressed electrotonically; (ii) *via* an action potential duration gradient and a conduction block zone, it promotes antegrade propagation of excitation from the SA node to the right atrium and prevents reentry of excitation; and (iii) *via* pacemaker shift, it allows pacemaking to continue under diverse pathophysiological circumstances." Functional importance of heterogeneity in cellular networks has been also demonstrated in theoretical studies. For example, presence of Ca clock in addition to membrane clock protects the SAN from annihilation which is associated with sinus node arrest [53]. The network structure critically determines oscillation regularity [59] and random parameter heterogeneity among oscillators can consistently rescue the system from losing synchrony [60].

Another possible advantage of cell specialization and heterogeneous signaling among SAN cells is more efficient energy consumption. For example, cells specializing in impulse conduction to atria, building aforementioned "conduction block zone", or generation of a particular rate may not possess a "powerful" Ca clock, consuming a lot of energy for its cAMP/PKA signaling [61], required for wide range rate regulation [26]. Furthermore, heterogeneous signaling in SAN tissue [8] implies that during rest many cells can stay in reserve, firing APs at lower rates (and not necessarily rhythmically), or even fall to dormancy, consuming much less energy. For example, in cats, the primary pacemaker consists of at most 2000 cells, but appears to function normally with less than 500 cells [62]. During fight-or-flight response, however, all reserves are recruited and maximally synchronized to generate rhythmic frequent impulses for maximum blood supply for the sake of survival at any energy cost.

Yet additional level of heterogeneity and complexity of cardiac pacemaker tissue is its intense innervation network [63-65] dubbed "little brain of the heart" [66] that provides precise control of SAN pacemaker cell function (*via* possible local control and guidance of heterogeneous signaling discussed above). SAN pacemaker cells also have interactions with non-excitable cells, such as telocytes [67,68] and fibroblasts [69] that could also aid in local control of heterogeneous signaling. Fibroblasts provides obstacles, ion current sinks or shunts to impulse conduction depending on their orientation, density, and coupling [50].

Supplementary Materials

Video S1: An example of classical type of βAR stimulation effects to decrease cycle length (i.e. to increase cycling rate). This 3.67 s video shows a 2D recording of Ca signals in basal state before stimulation. See Figure 1A.

Video S2: An example of classical type of βAR stimulation effects to decrease cycle length (i.e. to increase cycling rate). This 3.67 s video shows a 2D recording of Ca signals of the same SA node cell as in Video S1 in the presence of stimulation. See Figure 1B.

Video S3: An example of absence of notable βAR stimulation effect on cycle length. This 3.5 s video shows a 2D recording of Ca signals in basal state before stimulation. See Figure 1C.

Video S4: An example of absence of notable βAR stimulation effect on cycle length. This 3.5 s video shows a 2D recording of Ca signals in the presence of stimulation. See Figure 1D.

Video S5: An example of unusual βAR stimulation effect to increase cycle length (i.e. decrease cycling rate). This 3.67 s video shows a 2D recording of Ca signals in basal state before stimulation. See Figure 1E.

Video S6: An example of unusual βAR stimulation effect to increase cycle length (i.e. decrease cycling rate). This 3.67 s video shows a 2D recording of Ca signals in the presence of stimulation. See Figure 1F.

Video S7: An example of βAR stimulation effect to substantially decrease cycle length in a cell with extremely long cycle length in the basal state. This 5.96 s video shows a 2D recording of Ca signals in basal state before stimulation. See Figure 2A.

Video S8: An example of βAR stimulation effect to substantially decrease cycle length in a cell with extremely long cycle length in the basal state. This 5.96 s video shows a 2D recording of Ca signals in the presence of stimulation. See Figure 2B.

Author Contributions:

Conceptualization, VAM and EGL;

methodology, MSK, OM, VAM;

software, VAM;

validation, OM, VAM, EGL;

investigation, MSK, LAM, OM, VAM;

resources, EGL;

data curation, VAM;

formal analysis, LAM, MSK

writing—original draft preparation, MSK, VAM;

writing—review and editing, MSK, OM, LAM, EGL, VAM;

visualization, VAM, LAM;

supervision, EGL, VAM;

project administration, EGL.

All authors have read and agreed to the published version of the manuscript."

Funding: This work was supported by the Intramural Research Program of the NIH, National Institute on Aging

Institutional Review Board Statement: The study was conducted in accordance with NIH guidelines for the care and use of animals, protocol # 034-LCS-2019.

Informed Consent Statement: Not applicable.

Data Availability Statement: All data are available upon the request sent to the corresponding author (VAM).

Acknowledgments: The authors wish to acknowledge the assistance of Brice D. Ziman for skillful isolation of SAN cells.

Conflicts of Interest: The authors declare no conflict of interest. The funders had no role in the design of the study; in the collection, analyses, or interpretation of data; in the writing of the manuscript, or in the decision to publish the results.

Abbreviations

Abbreviation:

SAN = sinoatrial node

AP = action potential

LCR = local Ca release

βAR = β-adrenergic receptor

HCN4 = Hyperpolarization Activated Cyclic Nucleotide Gated Potassium Channel 4

I_f = the "Funny" current, a mixed Na-K inward HCN current activated by hyperpolarization

I_{CaL} = L-type Ca current

I_K = delayed rectifier K current

RyR2 = Ryanodine Receptor type 2

SERCA2 = sarco/endoplasmic reticulum Ca-ATPase type 2

Cycle length = action potential cycle length

cAMP = cyclic adenosine monophosphate

PKA = cAMP-dependent protein kinase type A

References

1. Mangoni, M.E.; Nargeot, J. Genesis and regulation of the heart automaticity. *Physiological reviews* **2008**, *88*, 919-982.
2. DiFrancesco, D. Pacemaker mechanisms in cardiac tissue. *Annual review of physiology* **1993**, *55*, 455-472, doi:10.1146/annurev.ph.55.030193.002323.
3. Nakayama, T.; Kurachi, Y.; Noma, A.; Irisawa, H. Action potential and membrane currents of single pacemaker cells of the rabbit heart. *Pflugers Arch* **1984**, *402*, 248-257.
4. Sano, T.; Sawanobori, T.; Adaniya, H. Mechanism of rhythm determination among pacemaker cells of the mammalian sinus node. *The American journal of physiology* **1978**, *235*, H379-384, doi:10.1152/ajpheart.1978.235.4.H379.
5. Bleeker, W.K.; Mackaay, A.J.; Masson-Pevet, M.; Bouman, L.N.; Becker, A.E. Functional and morphological organization of the rabbit sinus node. *Circulation research* **1980**, *46*, 11-22.
6. Jalife, J. Mutual entrainment and electrical coupling as mechanisms for synchronous firing of rabbit sino-atrial pacemaker cells. *The Journal of physiology* **1984**, *356*, 221-243.
7. Michaels, D.C.; Matyas, E.P.; Jalife, J. Mechanisms of sinoatrial pacemaker synchronization: a new hypothesis. *Circulation research* **1987**, *61*, 704-714.
8. Bychkov, R.; Juhaszova, M.; Tsutsui, K.; Coletta, C.; Stern, M.D.; Maltsev, V.A.; Lakatta, E.G. Synchronized cardiac impulses emerge from multi-scale, heterogeneous local calcium signals within and among cells of heart pacemaker tissue. *JACC Clin Electrophysiol* **2020**, *6*, 907-931, doi:10.1016/j.jacep.2020.06.022.
9. Fenske, S.; Hennis, K.; Rotzer, R.D.; Brox, V.F.; Becirovic, E.; Scharr, A.; Gruner, C.; Ziegler, T.; Mehlfeld, V.; Brennan, J.; et al. cAMP-dependent regulation of HCN4 controls the tonic entrainment process in sinoatrial node pacemaker cells. *Nat Commun* **2020**, *11*, 5555, doi:10.1038/s41467-020-19304-9.
10. Kim, M.S.; Maltsev, A.V.; Monfredi, O.; Maltseva, L.A.; Wirth, A.; Florio, M.C.; Tsutsui, K.; Riordon, D.R.; Parsons, S.P.; Tagirova, S.; et al. Heterogeneity of calcium clock functions in dormant, dysrhythmically and rhythmically firing single pacemaker cells isolated from SA node. *Cell calcium* **2018**, *74*, 168-179, doi:10.1016/j.ceca.2018.07.002.

11. Tsutsui, K.; Monfredi, O.; Sirenko-Tagirova, S.G.; Maltseva, L.A.; Bychkov, R.; Kim, M.S.; Ziman, B.D.; Tarasov, K.V.; Tarasova, Y.S.; Zhang, J.; et al. A coupled-clock system drives the automaticity of human sinoatrial nodal pacemaker cells. *Science signaling* **2018**, *11*, eaap7608.
12. Tsutsui, K.; Florio, M.C.; Yang, A.; Wirth, A.N.; Yang, D.; Kim, M.S.; Ziman, B.D.; Bychkov, R.; Monfredi, O.J.; Maltsev, V.A.; et al. cAMP-Dependent Signaling Restores AP Firing in Dormant SA Node Cells via Enhancement of Surface Membrane Currents and Calcium Coupling. *Front Physiol* **2021**, *12*, 596832, doi:10.3389/fphys.2021.596832.
13. Maltsev, V.A.; Lakatta, E.G. Synergism of coupled subsarcolemmal Ca^{2+} clocks and sarcolemmal voltage clocks confers robust and flexible pacemaker function in a novel pacemaker cell model. *American journal of physiology* **2009**, *296*, H594-H615.
14. Lakatta, E.G.; Maltsev, V.A.; Vinogradova, T.M. A coupled SYSTEM of intracellular Ca^{2+} clocks and surface membrane voltage clocks controls the timekeeping mechanism of the heart's pacemaker. *Circulation research* **2010**, *106*, 659-673.
15. Lyashkov, A.E.; Behar, J.; Lakatta, E.G.; Yaniv, Y.; Maltsev, V.A. Positive Feedback Mechanisms among Local Ca Releases, NCX, and ICaL Ignite Pacemaker Action Potentials. *Biophysical journal* **2018**, *114*, 1176-1189, doi:10.1016/j.bpj.2017.12.043.
16. Yaniv, Y.; Ganesan, A.; Yang, D.; Ziman, B.D.; Lyashkov, A.E.; Levchenko, A.; Zhang, J.; Lakatta, E.G. Real-time relationship between PKA biochemical signal network dynamics and increased action potential firing rate in heart pacemaker cells: Kinetics of PKA activation in heart pacemaker cells. *Journal of molecular and cellular cardiology* **2015**, *86*, 168-178, doi:10.1016/j.yjmcc.2015.07.024.
17. Musa, H.; Lei, M.; Honjo, H.; Jones, S.A.; Dobrzynski, H.; Lancaster, M.K.; Takagishi, Y.; Henderson, Z.; Kodama, I.; Boyett, M.R. Heterogeneous expression of Ca^{2+} handling proteins in rabbit sinoatrial node. *J Histochem Cytochem* **2002**, *50*, 311-324.
18. Honjo, H.; Boyett, M.R.; Kodama, I.; Toyama, J. Correlation between electrical activity and the size of rabbit sino-atrial node cells. *The Journal of physiology* **1996**, *496 (Pt 3)*, 795-808.
19. Monfredi, O.; Tsutsui, K.; Ziman, B.; Stern, M.D.; Lakatta, E.G.; Maltsev, V.A. Electrophysiological heterogeneity of pacemaker cells in the rabbit intercaval region, including the SA node: insights from recording multiple ion currents in each cell. *American journal of physiology* **2018**, *314*, H403-H414, doi:10.1152/ajpheart.00253.2016.
20. Vinogradova, T.M.; Zhou, Y.Y.; Maltsev, V.; Lyashkov, A.; Stern, M.; Lakatta, E.G. Rhythmic ryanodine receptor Ca^{2+} releases during diastolic depolarization of sinoatrial pacemaker cells do not require membrane depolarization. *Circulation research* **2004**, *94*, 802-809.
21. Monfredi, O.; Maltseva, L.A.; Spurgeon, H.A.; Boyett, M.R.; Lakatta, E.G.; Maltsev, V.A. Beat-to-beat variation in periodicity of local calcium releases contributes to intrinsic variations of spontaneous cycle length in isolated single sinoatrial node cells. *PLoS One* **2013**, *8*, e67247.
22. Yaniv, Y.; Stern, M.D.; Lakatta, E.G.; Maltsev, V.A. Mechanisms of beat-to-beat regulation of cardiac pacemaker cell function by Ca^{2+} cycling dynamics. *Biophysical journal* **2013**, *105*, 1551-1561.
23. Maltsev, A.V.; Parsons, S.P.; Kim, M.S.; Tsutsui, K.; Stern, M.D.; Lakatta, E.G.; Maltsev, V.A.; Monfredi, O. Computer algorithms for automated detection and analysis of local Ca^{2+} releases in spontaneously beating cardiac pacemaker cells. *PLoS One* **2017**, *12*, e0179419.
24. Vinogradova, T.M.; Bogdanov, K.Y.; Lakatta, E.G. beta-Adrenergic stimulation modulates ryanodine receptor Ca^{2+} release during diastolic depolarization to accelerate pacemaker activity in rabbit sinoatrial nodal cells. *Circulation research* **2002**, *90*, 73-79.

25. Lyashkov, A.E.; Juhaszova, M.; Dobrzynski, H.; Vinogradova, T.M.; Maltsev, V.A.; Juhasz, O.; Spurgeon, H.A.; Sollott, S.J.; Lakatta, E.G. Calcium cycling protein density and functional importance to automaticity of isolated sinoatrial nodal cells are independent of cell size. *Circulation research* **2007**, *100*, 1723-1731
26. Maltsev, V.A.; Lakatta, E.G. Numerical models based on a minimal set of sarcolemmal electrogenic proteins and an intracellular Ca clock generate robust, flexible, and energy-efficient cardiac pacemaking. *Journal of molecular and cellular cardiology* **2013**, *59*, 181-195.
27. Nivala, M.; Ko, C.Y.; Nivala, M.; Weiss, J.N.; Qu, Z. Criticality in intracellular calcium signaling in cardiac myocytes. *Biophysical journal* **2012**, *102*, 2433-2442.
28. Maltsev, A.V.; Maltsev, V.A.; Mikheev, M.; Maltseva, L.A.; Sirenko, S.G.; Lakatta, E.G.; Stern, M.D. Synchronization of stochastic Ca^{2+} release units creates a rhythmic Ca^{2+} clock in cardiac pacemaker cells. *Biophysical journal* **2011**, *100*, 271-283.
29. Weiss, J.N.; Qu, Z. The Sinus Node: Still Mysterious After All These Years. *JACC Clin Electrophysiol* **2020**, *6*, 1841-1843, doi:10.1016/j.jacep.2020.09.017.
30. Bak, P. *How Nature Works: the science of self-organized criticality*; Springer-Verlag: New York, 1999.
31. Yang, D.; Morrell, C.H.; Lyashkov, A.E.; Tagirova, S.; Zahanich, I.; Yaniv, Y.; Vinogradova, T.; Ziman, B.; Maltsev, V.A.; Lakatta, E.G. Ca2+ and Membrane Potential Transitions During Action Potentials are Self-Similar to Each Other and to Variability of AP Firing Intervals Across the Broad Physiologic Range of AP Intervals During Autonomic Receptor Stimulation. *Front Physiol* **2021**, *in print*, doi:DOI: 10.3389/fphys.2021.612770.
32. Tagirova Sirenko, S.; Tsutsui, K.; Tarasov, K.V.; Yang, D.; Wirth, A.N.; Maltsev, V.A.; Ziman, B.D.; Yaniv, Y.; Lakatta, E.G. Self-Similar Synchronization of Calcium and Membrane Potential Transitions During Action Potential Cycles Predict Heart Rate Across Species. *JACC Clin Electrophysiol* **2021**, doi:10.1016/j.jacep.2021.02.016.
33. Lyashkov, A.E.; Vinogradova, T.M.; Zahanich, I.; Li, Y.; Younes, A.; Nuss, H.B.; Spurgeon, H.A.; Maltsev, V.A.; Lakatta, E.G. Cholinergic receptor signaling modulates spontaneous firing of sinoatrial nodal cells via integrated effects on PKA-dependent Ca^{2+} cycling and I_{KACh}. *American journal of physiology* **2009**, *297*, H949-H959.
34. Lang, D.; Glukhov, A.V. Functional Microdomains in Heart's Pacemaker: A Step Beyond Classical Electrophysiology and Remodeling. *Front Physiol* **2018**, *9*, 1686, doi:10.3389/fphys.2018.01686.
35. Younes, A.; Lyashkov, A.E.; Graham, D.; Sheydina, A.; Volkova, M.V.; Mitsak, M.; Vinogradova, T.M.; Lukyanenko, Y.O.; Li, Y.; Ruknudin, A.M.; et al. Ca^{2+}-stimulated basal adenylyl cyclase activity localization in membrane lipid microdomains of cardiac sinoatrial nodal pacemaker cells. *The Journal of biological chemistry* **2008**, *283*, 14461-14468.
36. Dokos, S.; Celler, B.G.; Lovell, N.H. Vagal control of sinoatrial rhythm: a mathematical model. *Journal of theoretical biology* **1996**, *182*, 21-44.
37. Demir, S.S.; Clark, J.W.; Giles, W.R. Parasympathetic modulation of sinoatrial node pacemaker activity in rabbit heart: a unifying model. *The American journal of physiology* **1999**, *276*, H2221-2244.
38. Zhang, H.; Holden, A.V.; Noble, D.; Boyett, M.R. Analysis of the chronotropic effect of acetylcholine on sinoatrial node cells. *J Cardiovasc Electrophysiol* **2002**, *13*, 465-474.
39. Himeno, Y.; Sarai, N.; Matsuoka, S.; Noma, A. Ionic mechanisms underlying the positive chronotropy induced by beta1-adrenergic stimulation in guinea pig sinoatrial node cells: a simulation study. *J Physiol Sci* **2008**, *58*, 53-65.
40. Maltsev, V.A.; Lakatta, E.G. A novel quantitative explanation for autonomic modulation of cardiac pacemaker cell automaticity via a dynamic system of sarcolemmal and intracellular proteins. *American journal of physiology* **2010**, *298*, H2010-H2023.

41. Yuan, X.; Ratajczyk, L.N.; Alvarado, F.; Valdivia, H.H.; Glukhov, A.V.; Lang, D. Hierarchical Pacemaker Clustering within the Rabbit Sinoatrial Node is Driven by Dynamic Interaction between the Components of the Coupled-Clock System. *Biophysical journal* **2020**, *118*, 345A (Abstract), doi:10.1016/j.bpj.2019.11.1994.
42. Brennan, J.A.; Chen, Q.; Gams, A.; Dyavanapalli, J.; Mendelowitz, D.; Peng, W.; Efimov, I.R. Evidence of Superior and Inferior Sinoatrial Nodes in the Mammalian Heart. *JACC Clin Electrophysiol* **2020**, *6*, 1827-1840, doi:10.1016/j.jacep.2020.09.012.
43. Opthof, T. Embryological development of pacemaker hierarchy and membrane currents related to the function of the adult sinus node: implications for autonomic modulation of biopacemakers. *Med Biol Eng Comput* **2007**, *45*, 119-132, doi:10.1007/s11517-006-0138-x.
44. Opthof, T.; VanGinneken, A.C.; Bouman, L.N.; Jongsma, H.J. The intrinsic cycle length in small pieces isolated from the rabbit sinoatrial node. *Journal of molecular and cellular cardiology* **1987**, *19*, 923-934.
45. Clancy, C.E.; Santana, L.F. Evolving Discovery of the Origin of the Heartbeat: A New Perspective on Sinus Rhythm. *JACC Clin Electrophysiol* **2020**, *6*, 932-934, doi:10.1016/j.jacep.2020.07.002.
46. Boyett, M.R.; Honjo, H.; Kodama, I. The sinoatrial node, a heterogeneous pacemaker structure. *Cardiovascular research* **2000**, *47*, 658-687.
47. Feldman, J.L.; Kam, K. Facing the challenge of mammalian neural microcircuits: taking a few breaths may help. *The Journal of physiology* **2015**, *593*, 3-23, doi:10.1113/jphysiol.2014.277632.
48. Zhang, H.; Holden, A.V.; Kodama, I.; Honjo, H.; Lei, M.; Varghese, T.; Boyett, M.R. Mathematical models of action potentials in the periphery and center of the rabbit sinoatrial node. *The American journal of physiology* **2000**, *279*, H397-421.
49. Cloherty, S.L.; Dokos, S.; Lovell, N.H. A comparison of 1-D models of cardiac pacemaker heterogeneity. *IEEE Trans Biomed Eng* **2006**, *53*, 164-177, doi:10.1109/TBME.2005.862538.
50. Oren, R.V.; Clancy, C.E. Determinants of heterogeneity, excitation and conduction in the sinoatrial node: a model study. *PLoS computational biology* **2010**, *6*, e1001041.
51. Huang, X.; Mi, Y.; Qian, Y.; Hu, G. Phase-locking behaviors in an ionic model of sinoatrial node cell and tissue. *Phys Rev E Stat Nonlin Soft Matter Phys* **2011**, *83*, 061917, doi:10.1103/PhysRevE.83.061917.
52. Glynn, P.; Onal, B.; Hund, T.J. Cycle length restitution in sinoatrial node cells: a theory for understanding spontaneous action potential dynamics. *PLoS One* **2014**, *9*, e89049, doi:10.1371/journal.pone.0089049.
53. Li, K.; Chu, Z.; Huang, X. Annihilation of the pacemaking activity in the sinoatrial node cell and tissue *AIP Advances* **2018**, *8*, 125319.
54. Gratz, D.; Onal, B.; Dalic, A.; Hund, T.J. Synchronization of pacemaking in the sinoatrial node: a mathematical modeling study. *Front Physics* **2018**, *6*, id.63, doi:doi.org/10.3389/fphy.2018.00063.
55. Mata, A.N.; Alonso, G.R.; Garza, G.L.; Fernández, J.R.G.; García, M.A.C.; Ábrego, N.P.C. Parallel simulation of the synchronization of heterogeneous cells in the sinoatrial node. *Concurrency Computat Pract Exper* **2019**, e5317, doi:DOI: 10.1002/cpe.5317.
56. Campana, C.A. 2-Dimensional Computational Model to Analyze the Effects of Cellular Heterogeinity on Cardiac Pacemaking. *PhD thesis, Bologna, Italy: Universita di Bologna, Corso di Studio in Ingegneria Biomedical* **2015**.
57. Munoz, M.A.; Kaur, J.; Vigmond, E.J. Onset of atrial arrhythmias elicited by autonomic modulation of rabbit sinoatrial node activity: a modeling study. *American journal of physiology* **2011**, *301*, H1974-1983, doi:10.1152/ajpheart.00059.2011.

58. Monfredi, O.; Lyashkov, A.E.; Johnsen, A.B.; Inada, S.; Schneider, H.; Wang, R.; Nirmalan, M.; Wisloff, U.; Maltsev, V.A.; Lakatta, E.G.; et al. Biophysical characterization of the underappreciated and important relationship between heart rate variability and heart rate. *Hypertension* **2014**, *64*, 1334-1343, doi:10.1161/HYPERTENSIONAHA.114.03782.
59. Kori, H.; Kawamura, Y.; Masuda, N. Structure of cell networks critically determines oscillation regularity. *Journal of theoretical biology* **2012**, *297*, 61-72, doi:10.1016/j.jtbi.2011.12.007.
60. Zhang, Y.; Ocampo-Espindola, J.L.; Kiss, I.Z.; Motter, A.E. Random heterogeneity outperforms design in network synchronization. *Proceedings of the National Academy of Sciences of the United States of America* **2021**, *118*, doi:10.1073/pnas.2024299118.
61. Yaniv, Y.; Juhaszova, M.; Lyashkov, A.E.; Spurgeon, H.A.; Sollott, S.J.; Lakatta, E.G. Ca^{2+}-regulated-cAMP/PKA signaling in cardiac pacemaker cells links ATP supply to demand. *Journal of molecular and cellular cardiology* **2011**, *51*, 740-748.
62. Opthof, T.; de Jonge, B.; Masson-Pevet, M.; Jongsma, H.J.; Bouman, L.N. Functional and morphological organization of the cat sinoatrial node. *Journal of molecular and cellular cardiology* **1986**, *18*, 1015-1031.
63. Pauza, D.H.; Rysevaite, K.; Inokaitis, H.; Jokubauskas, M.; Pauza, A.G.; Brack, K.E.; Pauziene, N. Innervation of sinoatrial nodal cardiomyocytes in mouse. A combined approach using immunofluorescent and electron microscopy. *Journal of molecular and cellular cardiology* **2014**, *75*, 188-197, doi:10.1016/j.yjmcc.2014.07.016.
64. Inokaitis, H.; Pauziene, N.; Rysevaite-Kyguoliene, K.; Pauza, D.H. Innervation of sinoatrial nodal cells in the rabbit. *Ann Anat* **2016**, *205*, 113-121, doi:10.1016/j.aanat.2016.03.007.
65. Anderson, R.H. The disposition, morphology and innervation of cardiac specialized tissue in the guinea-pig. *J Anat* **1972**, *111*, 453-468.
66. Armour, J.A. Potential clinical relevance of the 'little brain' on the mammalian heart. *Exp Physiol* **2008**, *93*, 165-176, doi:10.1113/expphysiol.2007.041178.
67. Mitrofanova, L.B.; Gorshkov, A.N.; Konovalov, P.V.; Krylova, J.S. Telocytes in the human sinoatrial node. *J Cell Mol Med* **2018**, *22*, 521-532, doi:10.1111/jcmm.13340.
68. Kondo, A.; Kaestner, K.H. Emerging diverse roles of telocytes. *Development* **2019**, *146*, doi:10.1242/dev.175018.
69. Camelliti, P.; Green, C.R.; LeGrice, I.; Kohl, P. Fibroblast network in rabbit sinoatrial node: structural and functional identification of homogeneous and heterogeneous cell coupling. *Circulation research* **2004**, *94*, 828-835, doi:10.1161/01.RES.0000122382.19400.14.